

Fig 1 Pitch-rate problem

decision, the remaining decisions must constitute an optimal policy with regard to the state resulting from the first decision

This means, in our problem, that, wherever the first  $(NP - 1)$  partitions have been placed, the  $NP$ th partition must be located so as to minimize the sum

$$\sum_{k=0}^{NP-1} \int_{\bar{x}_k}^{\bar{x}_{k+1}} [y(x) - \alpha_k]^2 dx + \int_{\bar{x}_{NP}}^{x_b} [y(x) - \alpha_{NP}]^2 dx$$

We are thus led to the recurrence relations

$$f_k(x_i) = \min_{x_a \leq x_j \leq x_i} [f_{k-1}(x_j) + A(x_j, x_i)] \quad (k = NP, NP - 1, \dots, 2, 1)$$

$$f_0(x_i) = A(x_a, x_i)$$

where  $A(x_j, x_i)$  is defined in Eq (2). The functions  $f_k(x_i)$  are computed for  $x_a \leq x_i \leq x_b$  and  $k = 0, 1, 2, \dots, NP$ . The values of  $x_j$  which minimize the quantities in brackets are also recorded and denoted by  $\bar{x}_k(x_i)$ ,  $k = 1, 2, \dots, NP$ . Then the optimal partition locations are given by  $\bar{x}_{NP} = \bar{x}_{NP}(x_b)$ ,  $\bar{x}_{NP-1} = \bar{x}_{NP-1}(\bar{x}_{NP})$ ,  $\bar{x}_2 = \bar{x}_2(\bar{x}_3)$ ,  $\bar{x}_1 = \bar{x}_1(\bar{x}_2)$ .

Once the optimal values of the  $\bar{x}_k$  are known, then we can use Eq (1) to find the optimal  $\alpha_k$ .

### Computational Aspects

A computer program that performs the functional approximation described in the previous section is available from the author<sup>5</sup>. The program assumes that the function  $y(x)$  is available as a discrete set of  $n$  values.

The computations are such that the desired information  $(\alpha_k, k = 0, \dots, NP; \bar{x}_k, k = 1, \dots, NP)$  is readily available for all  $NP$  less than the desired value, and all of these results are provided by the program. The errors, i.e., the values of  $f_{NP}(x_b)$  are also provided.

All integrations are performed using the trapezoid rule, i.e.,  $y(x)$  is assumed to be linear between the discrete points at which it is given. A less simple, more accurate, quadrature formula could be used if additional accuracy were required for some application.

It should also be noted that the optimal partition locations must be chosen from among the  $n$  discrete points at which  $y(x)$  is specified. The errors introduced by this approximation remain negligible as long as  $n$  is relatively large compared to  $NP$ . The actual magnitude of these errors can be examined by referring to simple problems for which an exact solution is available<sup>5</sup>.

### Example

A typical desired pitch-rate program for a rocket stage is shown in Fig 1. The function is discontinuous, consisting of an initial kick followed by a gravity turn. For tech-

nological reasons, it is often necessary to follow a series of steps rather than attempting to follow the theoretical curve exactly. Then it is of interest to have the step curve as close as possible to the theoretical curve.

This particular problem (for  $NP \leq 50$  and  $n = 91$ ) required less than 2 min on the IBM 7094 computer. The solution for  $NP = 2$  is drawn on Fig 1 for comparison with the theoretical curve.

### References

- Stone, H., Approximation of curves by line segments," *Math Computation* **15**, 40-47 (1961).
- Bellman, R. E. and Kotkin, B., "On the approximation of curves by line segments using dynamic programming—II," Rand Corp RM-2978-PR, Armed Services Tech Info Agency AD272 143 (February 1962).
- Cerrillo, M. V. and Guillemin, E. A., "On basic existence theorems III. Theoretical considerations on rational fraction expansions for network functions," Mass Inst Tech Res Lab of Electronics, TR 233 (June 4, 1952).
- Bellman, R. E. and Dreyfus, S. E., *Applied Dynamic Programming* (Princeton University Press, Princeton, N. J., 1962), p 15.
- Lubowe, A. G., "Optimal functional approximation using dynamic programming," Bell Telephone Labs Internal Memo (August 15, 1963).

## Flutter of Two Parallel Flat Plates Connected by an Elastic Medium

JOHN A. McELMAN\*

NASA Langley Research Center, Hampton, Va

### Nomenclature

$A_{\pm}$	$= R_{x_{\pm}} - 2(a/b)^2$
$a, b$	$=$ plate length and width, see Fig 1
$B_{\pm}$	$= (\Omega_{\pm}^2/\pi^4) + (a/b)^2 R_{y_{\pm}} - (a/b)^4$
$D_{\pm}$	$=$ plate flexural stiffness
$h_{\pm}$	$=$ thickness of plate
$k$	$=$ elastic spring constant
$l$	$=$ lateral aerodynamic load
$M$	$=$ Mach number
$N_{x_{\pm}}, N_{y_{\pm}}$	$=$ midplane force intensities, positive in compression
$q$	$=$ dynamic pressure, $\rho U^2/2$
$R_{x_{\pm}}$	$= a^2 N_{x_{\pm}}/\pi^2 D_{\pm}$
$R_{y_{\pm}}$	$= a^2 N_{y_{\pm}}/\pi^2 D_{\pm}$
$S_{\pm}$	$=$ spring stiffness parameter, $ka^4/\pi^4 D_{\pm}$
$t$	$=$ time
$U$	$=$ freestream velocity
$w_{\pm}$	$=$ lateral deflection of plate
$x, y$	$=$ Cartesian coordinates see Fig 1
$\beta$	$= (M^2 - 1)^{1/2}$
$\gamma_{\pm}$	$=$ mass density of plate
$\lambda$	$= 2qa^3/\beta D_{\pm}$
$\rho$	$=$ mass density of air
$\omega$	$=$ circular frequency
$\Omega_{\pm}^2$	$= \omega^2 a^4 \gamma_{\pm} h_{\pm}/D_{\pm}$
$+$ -	$=$ subscripts refer to upper and lower plate, respectively

### Introduction

THE flutter behavior of a structural configuration consisting of two rectangular, simply supported, parallel plates laterally connected by many closely spaced linear springs is investigated. The configuration analyzed is shown in Fig 1. The upper plate has air flowing at supersonic speed over the

Received October 25 1963

\* Aerospace Engineer

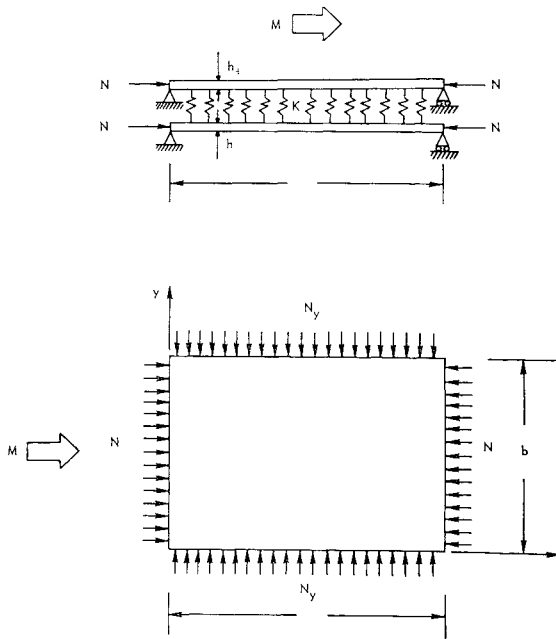


Fig 1 Configuration and coordinate system

upper surface, and both plates are subjected to midplane loadings

This configuration is an idealization of a micrometeoroid bumper that is attached to a primary structure by a light, soft filler material. The aeroelastic behavior of such a configuration may be important in the design of structural components of a manned space station which are exposed to an airstream during launch.

#### Analysis

The equilibrium equations and appropriate boundary conditions are

$$D_+ \nabla^4 w_+ + N_{x+} \frac{\partial^2 w_+}{\partial x^2} + N_{y+} \frac{\partial^2 w_+}{\partial y^2} + \gamma_+ h_+ \frac{\partial^2 w_+}{\partial t^2} + k(w_+ - w_-) = l(x, y, t) \quad (1)$$

$$D_- \nabla^4 w_- + N_{x-} \frac{\partial^2 w_-}{\partial x^2} + N_{y-} \frac{\partial^2 w_-}{\partial y^2} + \gamma_- h_- \frac{\partial^2 w_-}{\partial t^2} + k(w_- - w_+) = 0 \quad (2)$$

$$\left. \begin{aligned} w_{\pm}(x, 0, t) &= w_{\pm}(x, b, t) = w_{\pm}(0, y, t) = w_{\pm}(a, y, t) = 0 \\ \frac{\partial^2 w_{\pm}}{\partial y^2}(x, 0, t) &= \frac{\partial^2 w_{\pm}}{\partial y^2}(x, b, t) = \frac{\partial^2 w_{\pm}}{\partial x^2}(0, y, t) = \frac{\partial^2 w_{\pm}}{\partial x^2}(a, y, t) = 0 \end{aligned} \right\} \quad (3)$$

$$\left| \begin{aligned} 1 - A_+ - B_+ + S_+ - \frac{S_+ S_-}{1 - A_- - B_- + S_-} \\ \frac{8 \lambda}{3 \pi^4} \end{aligned} \right|$$

where  $l(x, y, t)$  is the lateral load per unit area due to aerodynamic pressure. For static strip theory the lateral load is given by the simple Ackeret value  $l(x, y, t) = -(2q/\beta) \times (\partial w_+ / \partial x)$ .

A two-term Galerkin solution is pursued. Solutions that satisfy the boundary conditions for simply supported edges are assumed as follows:

$$w_{\pm}(x, y, t) = \left[ C_{1\pm} \sin\left(\frac{\pi x}{a}\right) \sin\left(\frac{\pi y}{b}\right) + C_{2\pm} \sin\left(\frac{2\pi x}{a}\right) \sin\left(\frac{\pi y}{b}\right) \right] e^{i\omega t} \quad (4)$$

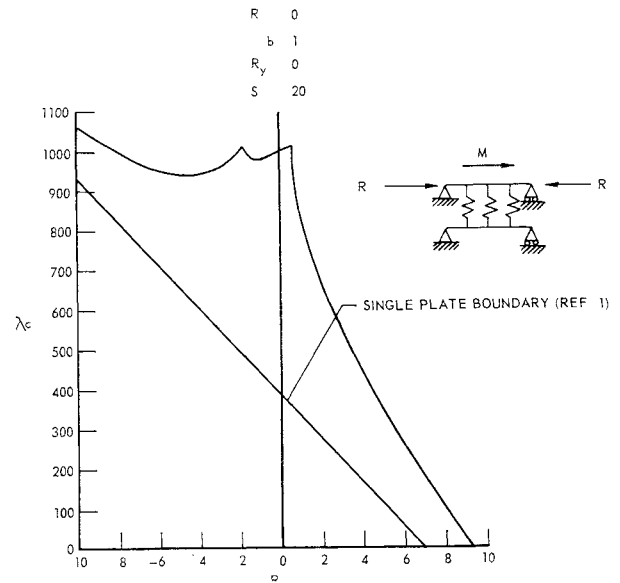


Fig 2 Flutter boundary for  $R_{x-} = 0$

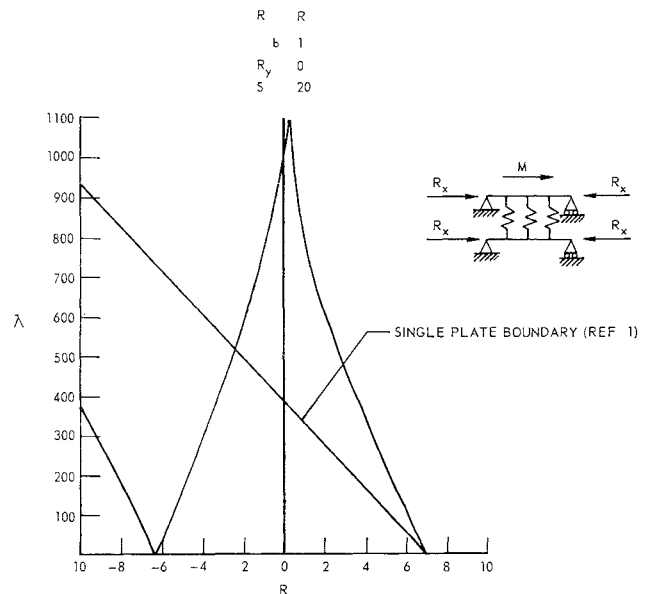


Fig 3 Flutter boundary for  $R_{x+} = R_{x-} = R_x$

The frequency  $\omega$  is, in general, complex; however, attention is directed primarily to real values for which the motion is harmonic.

When Eq (4) is substituted into Eqs (1) and (2) and the Galerkin procedure is used, the following equation is obtained:

$$\left| \begin{aligned} -\frac{8 \lambda}{3 \pi^4} \\ 16 - 4A_+ - B_+ + S_+ - \frac{S_+ S_-}{16 - 4A_- - B_- + S_-} \end{aligned} \right| = 0 \quad (5)$$

Flutter occurs with the coalescence of two natural frequencies as the dynamic pressure parameter  $\lambda$  increases (see Ref 1). The procedure is to solve Eq (5) for  $\lambda$  and maximize the resulting expression with respect to the frequency to obtain a critical value of the dynamic pressure parameter  $\lambda_{cr}$ . In many cases, more than one critical value exists corresponding to the coalescence of different pairs of modes, and it is necessary to seek the lowest critical value to define a flutter boundary.

In order to illustrate the general flutter characteristics exhibited by this configuration, calculations were made for the simplified case for which  $h_+ = h_-$ ,  $D_+ = D_-$ ,  $R_{y\pm} = 0$ ,  $a/b$

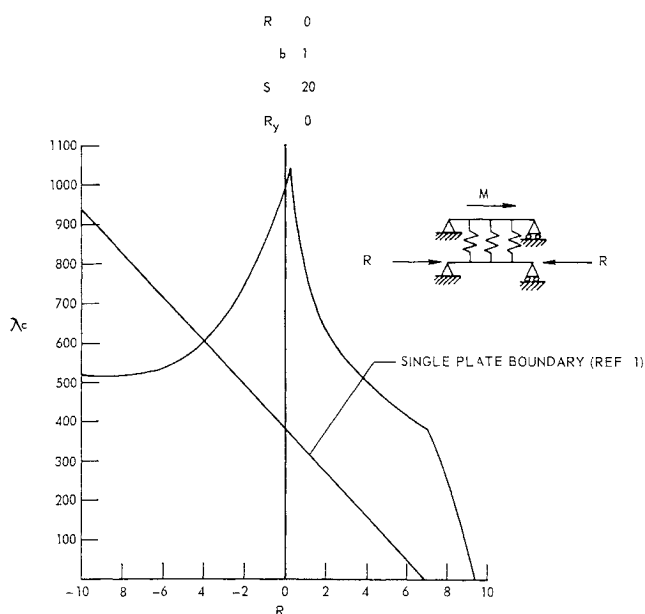


Fig 4 Flutter boundary for  $R_{x+} = 0$

$= 1$ , and  $S_+ = S_- = S$ . Flutter boundaries were derived from Eq (5) for several combinations of streamwise midplane loads in the two plates. It must be remembered that these boundaries are subject to the same limitations that are described in Ref 1; in particular, the range of validity of the boundaries is limited by the buckling characteristics of the plates.

#### Discussion

For a single flat isotropic plate, the flutter boundary as determined from a two-term Galerkin solution is a linear function of the midplane load in the streamwise direction. Because of the coupling of the motions of the two plates, however, the configuration analyzed herein exhibits entirely different boundaries. Peaks and valleys occur in the boundaries because the system can be tuned by means of the midplane loads.

Figures 2-4 present flutter boundaries ( $\lambda_{cr}$  vs  $R_x$ ) for square plates having various combinations of midplane loads and a spring parameter of  $S = 20$ . At the present time realistic values of  $S$  are not clearly defined; the value chosen ( $S = 20$ ) might be typical of a configuration with a very soft filler material. The flutter boundary for a single flat plate with the same physical properties as either the upper or the lower plate considered in the present analysis is also shown in each of the figures (see Ref 1).

Figure 2 is a plot of the boundary for the configuration when there is no load in the lower plate. This boundary becomes asymptotic to the single plate boundary for large negative values of  $R_x$ , i.e., large midplane tension, as do all of the boundaries considered herein.

Figure 3 is a plot of the boundary when the midplane loads are the same in each plate. Here the tuning effect can be very significant since it is possible to have a zero flutter speed with a tensile load, and a peak exists which is much higher than the corresponding value for the single plate.

Figure 4 is a plot of the boundary when there is no load in the upper plate. This case is perhaps the most realistic combination of loading if the configuration is considered to be a micrometeoroid protection device. This boundary has characteristics very similar to the boundary in Fig 2 except that here the tuning effect is more prevalent. In particular, for streamwise tension, a condition that can be expected from bending loads on a space vehicle during launch, the elastically supported plate is more prone to flutter than the single plate alone.

The results of this analysis indicate that if a configuration similar to this one is used for applications where supersonic airflows are encountered, a very careful flutter analysis is in order to insure that undesirable flutter characteristics are not present.

#### Reference

- <sup>1</sup> Hedgepeth, J. M., "Flutter of rectangular simply supported panels at high supersonic speeds," *J. Aeronaut. Sci.* **24**, 563-573 (1957).

## Re-Entry Heat Conduction of a Finite Slab with a Nonconstant Thermal Conductivity

WILLIAM R. WELLS\*

NASA Langley Research Center, Hampton, Va

The intense temperatures at the surface of a space vehicle may, in some instances, alter the thermal conductivity of the layers of the skin below the surface. This analysis presents, as a first approximation to the problem, a closed-form solution for the case of a thermal conductivity that varies linearly with distance below the surface. A convective heat input at the surface which is exponential in time is assumed. The results should apply for the initial phases of entry in which the entry velocity and angle are nearly constant.

#### Nomenclature

- $a$  = slope of thermal conductivity curve
- $B$  = constant that depends on entry velocity and angle
- $c$  = specific heat of material
- $C_1, C_2$  = arbitrary constants
- $i$  =  $-1^{1/2}$ , imaginary unit
- $I_0, I_1$  = modified Bessel functions of the first kind of order, zero and one, respectively
- $J_0, J_1$  = Bessel functions of the first kind of order, zero and one, respectively
- $K$  = thermal conductivity
- $K_0, K_1$  = modified Bessel functions of the second kind of order, zero and one, respectively
- $s$  = variable in the Laplace transform
- $t$  = time measured from entry
- $T, \bar{T}$  = temperature and transformed temperature, respectively
- $V$  = entry velocity
- $x$  = distance normal to surface
- $Y_0, Y_1$  = Bessel functions of the second kind of order, zero and one, respectively
- $\gamma$  = entry angle
- $\theta$  =  $\rho c/a^2$
- $\rho$  = density of material
- $\tau$  = thickness of material
- $\omega$  = constant that depends on entry velocity and angle

#### Subscripts

- $i$  = initial conditions
- $f$  = final conditions

THE solution to the problem of one-dimensional heat conduction through a skin with constant thermal conductivity for the initial phases of a re-entry in which the velocity and entry angle are nearly constant and for which the convective heat rate is the dominant input can be found in Ref 1. The present analysis intends to take the basic

Received October 30, 1963

\* Aerospace Technologist, Space Mechanics Division